Modeled and satellite-derived extreme wave height statistics in the North Atlantic Ocean reaching 20 m

Takuji Waseda[1], Kaushik Sasmal[2], Tsubasa Kodaira[1], Yuki Kita[3], Rei Miratsu[4], Tingyao Zhu[4], and Tsutomu Fukui[4]

[1]University of Tokyo
[2]The University of Tokyo
[3]MS&AD InterRisk Research & Consulting, Inc.
[4]Nippon Kaiji Kyokai (ClassNK)

November 24, 2022

Abstract

Wave statistics of the North Atlantic Ocean, instrumental in designing merchant ships, were revisited by an in-house high-resolution 25-year wave hindcast (TodaiWW3-NK). The tail of the exceedance probability of H_s was extended to 20 m and compared surprisingly well against the satellite altimeter. Moreover, we have found that the largest storm event in 25 years with the highest wave over 21 m in January 2014 significantly enhanced the tail of the H_s distribution, which is a feature that was common among the three wave-hindcasts (ERA5/ECMWF, IOWAGA/IFREMER, and TodaiWW3-NK). Paradoxically, the satellite altimeter did not detect the H_s at the peak of this storm. We found that extreme wave heights from models and satellites of three storms in 2007, 2011, and 2014 may deviate about a few meters among the estimates, particularly the altimeter having a large uncertainty. In-situ observations of the extreme wave events are urgently in need.

Modeled and satellite-derived extreme wave height statistics in the North Atlantic Ocean reaching 20 m

Kaushik Sasmal[1], Tsubasa Kodaira[1], Yuki Kita[2], Rei Miratsu[3], Tingyao Zhu[3], Tsutomu Fukui[3], Takuji Waseda[1]

[1]Graduate School of Frontier Sciences, The University of Tokyo, Kashiwa, Chiba, Japan
[2]MS&AD InterRisk Research & Consulting, Inc., Chiyoda, Tokyo, Japan
[3]Nippon Kaiji Kyokai (ClassNK), Chiyoda, Tokyo, Japan

Key Points:

- The wave height statistics reaching 20 m were derived from 25-year wave hindcast and satellite-altimeter
- Inter-comparison of model, buoy and satellite revealed that uncertainty of satellite altimeter reaches a few meters.
- The 25-year wave statistics is dominated by a single event in 2014.

Corresponding author: Takuji Waseda, `waseda@k.u-tokyo.ac.jp`

Abstract

Wave statistics of the North Atlantic Ocean, instrumental in designing merchant ships, were revisited by an in-house high-resolution 25-year wave hindcast (TodaiWW3-NK). The tail of the exceedance probability of H_s was extended to 20 m and compared surprisingly well against the satellite altimeter. Moreover, we have found that the largest storm event in 25 years with the highest wave over 21 m in January 2014 significantly enhanced the tail of the H_s distribution, which is a feature that was common among the three wave-hindcasts (ERA5/ECMWF, IOWAGA/IFREMER, and TodaiWW3-NK). Paradoxically, the satellite altimeter did not detect the H_s at the peak of this storm. We found that extreme wave heights from models and satellites of three storms in 2007, 2011, and 2014 may deviate about a few meters among the estimates, particularly the altimeter having a large uncertainty. In-situ observations of the extreme wave events are urgently in need.

Plain Language Summary

Sea states in the North Atlantic Ocean is considered to be the severest among the basins with large ship traffic. Traditionally, the wave statistics in the North Atlantic Ocean were used to estimate the design loads of the ships. In this study, the wave statistics was reproduced based on numerical wave simulation of 1994 to 2018. The result was compared to the wave heights observed by satellites. They compare well up to almost 20 m wave height. However, we have found that the severest storm in 25 years registering 21 m and higher waves were not observed by satellites. This puzzling fact implies that the uncertainty of the satellite observation of the extreme wave events is large and has never been validated. We suggest enhancement of the in-situ observation of the extreme wave events.

1 Introduction

The sea states in the North Atlantic Ocean is considered to be the most severe among seas with heavy ship traffic. Therefore, the joint probability distribution of significant wave height (H_s) and wave period (T_z) (also referred to as scatter diagram) in the North Atlantic Ocean have been used to estimate wave loads which is a crucial factor for the structural design of ships (Cardone et al., 2015; Bitner-Gregersen et al., 2016). The scatter diagram is constructed based on ocean areas 8, 9, 15, and 16 of the Global Wave Statistics (GWS Hogben et al. (1986)) as recommended by the International Association of Classification Societies (IACS) Rec. 34, (see IACS. (2001)). The GWS database was derived from visual observations and may not include extreme wave heights caused by storms as the ships may have avoided navigating into the storms. Therefore, the existing GWS database does not represent extreme wave heights and the bias towards lower wave heights is corrected (Bitner-Gregersen et al., 2016).

In a recent study, a 23-year (1990-2012) hindcast dataset IOWAGA/IFREMER (Rascle & Ardhuin, 2013) was used to identify extreme wave regions in the North Atlantic Ocean by deriving spatial distribution of return periods of storms for a given H_s threshold value (Ponce de León et al., 2015). They found that the regions of extreme waves are associated with the storm tracks of tropical and extratropical cyclones. The North Atlantic Ocean experiences severe storms particularly during the winter months (December, January and February). Studies show that significant wave height (H_s) reached 20.0 m during several extreme events associated with rapidly intensifying extratropical cyclones (Cardone et al., 2011). The number of extratropical storms with hurricane force winds in the North Atlantic Ocean can exceed 10 per year (Hanafin et al., 2012).

There are two renowned extreme events observed by satellite altimeter. During an extreme event in 2011, the JASON-2 altimeter measured $H_s = 20.12$ m on February 14 at 11:03:09 UTC under the storm Quirin. This was "a record-breaking maximum value of H_s" according to Ardhuin et al. (2011). During another extreme event in 2007, the JASON-1

Ku-band altimeter measured H_s of 20.2 m on February 9, 2007, at 21:31 UTC (Cardone et al., 2009), which was reprocessed in NASA and CNES data to be 19.13 m (Ardhuin et al., 2011).

Within the 25-year analysis period (1994-2018) of our study, we found that a phenomenal storm occurred in the North Atlantic Ocean during January 4-6, 2014. The name Hércules (Ponce De León & Guedes Soares, 2015b) was given to this winter storm because of its unusual size and intensity. It is noteworthy that none of the four satellite altimeters (JASON-2, HY-2A, CRYOSAT-2, SARAL) operating at that time captured the extreme waves at the peak of the storm intensification. The JASON-2 altimeter, which has a repeat cycle of 10-day measured only up to $H_s = 15.5$ m, whereas SARAL recorded $H_s = 19.24$ m. However, none of these altimeter passes were close to the core of the storm. Therefore, the H_s extreme under Hércules is undetected by the altimeters.

The wave heights during extreme events are undetected not only by altimeters but by buoys as well (Alves & Young, 2003). Nevertheless, three large wave events were detected by the moored buoy network of the UK Met Office. At the K3 buoy (53.52^o N, 18.46^o W), H_s exceeding 18.0 m was registered during December 8-9 in 2007, and at the K2 buoy (51.00^o N, 13.35^o W), waves over 17.0 m H_s was registered on March 10, 2008 (Turton & Fenna, 2008). During another extreme event in 2013, the K5 buoy recorded a H_s of 19.0 m at 0600 UTC on February 4th, 2013 in the North Atlantic Ocean (59.11^o N, 11.70^o W). 19.0 m is the highest significant wave height measured by a buoy, according to WMO (https://public.wmo.int/en/media/press-release/19-meter-wave-sets-new-record-highest-significant-wave-height-measured-buoy). We present model validation for this extreme event by comparing two different hindcast datasets ERA5/ECWAM (Hersbach et al., 2020) and TodaiWW3-NK. The model validation for such H_s extremes has not been reported before.

In this paper, we revisit the wave statistics of GWS 8, 9, 15, and 16 areas in the North Atlantic Ocean by utilizing 25-year (1994-2018) wave hindcast data from our in-house TodaiWW3-NK. Our objective is to re-derive the marginal distribution of H_s in the GWS 8, 9, 15, and 16 areas from TodaiWW3-NK. The exceedance probability of H_s from TodaiWW3-NK is validated against satellite altimeter data and compared against other models, ERA5/ECMWF, and IOWAGA/IFREMER. The TodaiWW3-NK has the highest spatial and spectral resolutions. We demonstrate that the impact of one single storm event (January 2014) on 25-year wave statistics is outstanding and dominantly affects the distribution. We show a comparison of H_s among different wave datasets and observations from both altimeters and buoy during a few selected extreme events in the North Atlantic Ocean. In addition to this, we compare H_s during extreme events among satellite altimeter datasets obtained from different sources to highlight how the estimates deviate for the extremes.

2 Data and Methodology

We analyzed 25 years of reanalysis (ERA5) and hindcast (IOWAGA and TodaiWW3-NK) data for GWS 8, 9, 15 and 16 areas (Figure S1). TodaiWW3-NK model computational domain encompasses the Atlantic Ocean with the spatial resolution of 0.20^o $\times$ 0.25^o (Lat $\times$ Lon), 35 frequency bins and 36 directional bins. For model physics, the ST4 package of Ardhuin et al. (2010) was used. The model was forced by NCEP/CFSR hourly wind ((Saha et al., 2010, 2014)) and was integrated for 25 years in hindcast mode (1994-2018).

The spatial resolutions of ERA5 and IOWAGA are 0.36^o $\times$ 0.36^o and 0.5^o $\times$ 0.5^o, respectively. The spectral resolution of ERA5 and IOWAGA are 24 directional bins and 30 frequency bins, and 24 directional bins and 31 frequency bins, respectively. For IOWAGA, the WAVEWATCH III model was forced by either ECMWF or CFSR winds depending on the year. The ST4 physics (Ardhuin et al., 2010) is employed in which the wind-wave growth parameter β_{max} was adjusted for different wind products to correct the average to higher wave heights (Ardhuin et al., 2011); $\beta_{max} = 1.52$ for ECMWF winds and $\beta_{max} = 1.33$ for CFSR winds.

For IOWAGA, no assimilation of the observed data was made, however, the model parameters were calibrated based on observations from buoys, satellite altimeters, SAR, and seismic noise spectra for years after 2008 (Ardhuin et al., 2011). For TodaiWW3-NK, no assimilation of observed data was made in the WAVEWATCH III model. The model was configured with ST4 physics package and forced by CFSR winds (Saha et al., 2010, 2014) with $\beta_{max} = 1.33$. The wave data in ERA5 were derived from ECWAM, which was forced by the winds from the ECMWF's coupled model system (IFS). Satellite altimeter data are assimilated in ERA5 for correction of H_s.

The exceedance probability was calculated as $\mathrm{r}/(n+1)$ based on the 25 years H_s data, where r is the rank, and n is the total number of data. We used this method to calculate the exceedance probability of H_s from satellite altimeter data as well. Here, we used the satellite altimeter data of Ribal and Young (2019); 33 years (1985-2018) of satellite data from 13 altimeters have been calibrated and quality controlled. They performed cross-calibration of H_s between different altimeters up to $H_s = 10.0$ m but did not guarantee the performance for the waves with $H_s > 10.0$ m. Upon comparing the exceedance probability between models and observations, we separated the altimeter data into two groups based on their repeat cycle; the altimeters with a repeat cycle of 10 days (TOPEX, JASON-1, JASON-2, and JASON-3) and the altimeters with a repeat cycle greater than or equal to 25 days (ERS-2, ENVISAT, CRYOSAT-2, SARAL, and SENTINEL-3A).

3 Results and Discussion

3.1 Exceedance probability of H_s from model and altimeter up to 20 m

Exceedance probabilities of H_s are estimated from the wave models and satellite altimeter data. The H_s data extracted from altimeters with a 10-day repeat cycle agree surprisingly well with TodaiWW3-NK data to approximately 18.5 m (Figure 1a). The tails of both distributions reach over 20 m, considerably extending the wave statistics from 16 m derived from visual observation in the GWS 8, 9, 15, and 16 regions. In this comparison, the coincidence of the satellite measurements and the model estimates are neglected. Therefore, tracks of TOPEX, JASON-1, JASON-2, and JASON-3 located within GWS 8, 9, 15, and 16 were all included. That is equivalent to applying an ergodic hypothesis in both space and time.

The reason why we used only the TOPEX, JASON-1, JASON-2, and JASON-3 derived H_s is because the altimeters with a 10-day repeat cycle are likely to capture more extremes compared to that with repeat cycle ≥ 25 days. The altimeter based distributions deviate from one another for $H_s > 7.0 - 8.0$ m (Figure S2). The tails of the distributions differ by more than 1.0 m between these two altimeter datasets. This comparison indicates that the H_s extremes (e.g., $H_s > 19.0$ m) might have gone undetected by the altimeters with repeat cycle ≥ 25 days due to under-sampling. Therefore, the higher sampling of altimeters with repeat cycle =10 days is the reason the altimeter derived H_s shows good agreement with that of the high-resolution model TodaiWW3-NK (Figure 1a).

The comparison of the exceedance probabilities of TodaiWW3-NK and satellite altimeter derived H_s is encouraging, but the comparison neglects the coincidence of the observation. It is anticipated that the locations and timings of the storm events have phase shifts, and therefore, the collocated observations may not match. From the collocated comparison of TodaiWW3-NK and altimeter derived H_s along satellite tracks of TOPEX, JASON-1, JASON-2, and JASON-3, we have found that the altimeter data tend to overestimate the H_s over 15.0 m. The conjecture derives from the inspection of a Q-Q plot and the corresponding exceedance probabilities of H_s (Figure S3). Overall, the correlation is 0.97, with almost

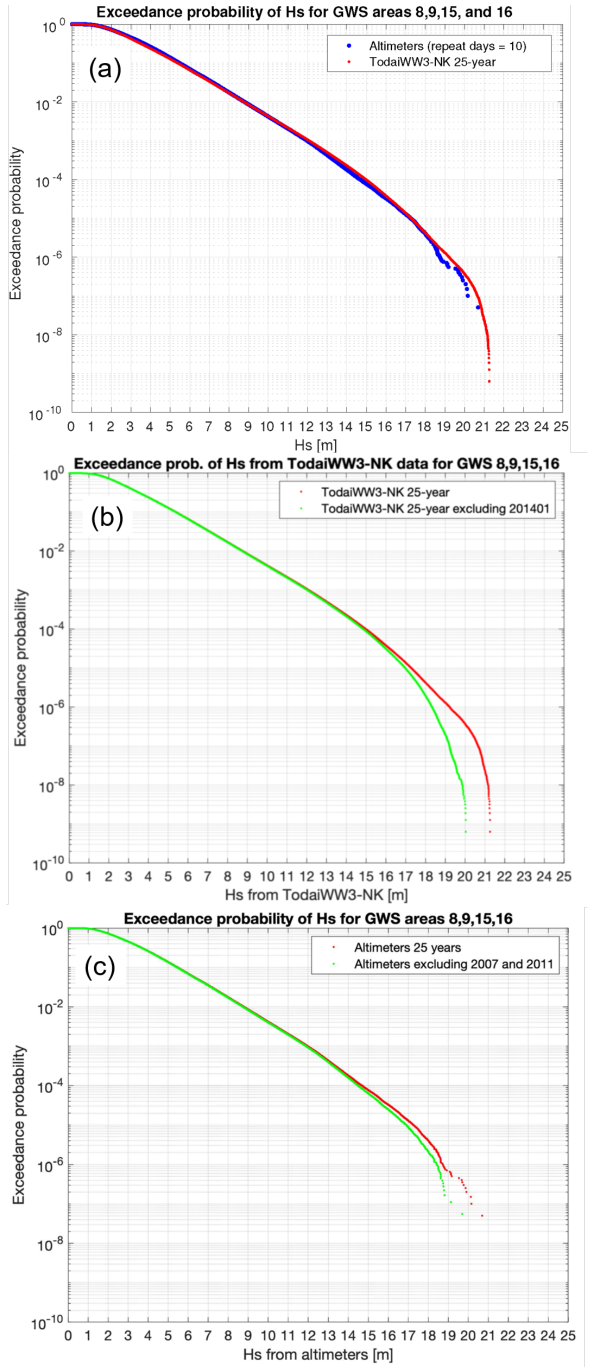

Figure 1. (a) Comparison of exceedance probability of significant wave height between model and altimeters. The altimeters with repeat days = 10 are TOPEX, JASON-1, JASON-2, and JASON-3. The comparison is made for GWS areas 8,9,15 and 16 using 25 years data from 1994 to 2018. The vertical axis is in log scale and the horizontal axis is in linear scale. (b) Exceedance probability of H_s from TodaiWW3-NK using 25 year 3-hourly data from 1994 to 2018 for GWS areas 8, 9, 15 and 16. The exceedance probability of H_s is compared with and without January 2014 data. (c) Exceedance probability of H_s from JASON-2 are compared using 25 year records from 1994 to 2018 within GWS areas 8, 9, 15 and 16, with and without 2014 and 2017 storm data.

negligible bias, root-mean-squared-error (RMSE) of 0.45 m, and a scatter index (SI) of 0.14, but they start to deviated beyond $H_s = 15.0$ m. Moreover, the tails of the distributions are quite different for $H_s > 19.0$ m.

Nevertheless, the agreement of wave model and satellite altimetry up to 15 m H_s is remarkable as altimeter-derived H_s has only been validated up to 10 m or so (Ribal & Young, 2019). The model is not perfect. However, we conclude that the spatial and spectral resolutions of the model are key parameters affecting the reproducibility of the extreme wave events, and, therefore, the TodaiWW3-NK is a suitable model to study the wave extremes. The exceedance probabilities from the three independent models were compared. For example, the values of H_s at exceedance probability of 10^{-8} are roughly 19.8 m, 20.3 m, and 21.1 m from ERA5, IOWAGA, and TodaiWW3-NK, respectively (Figure S4). Considering that the only difference between TodaiWW3-NK and IOWAGA is the spatial and the spectral resolutions (see section 2), and neither the model physics nor the wind forcing, we may conclude that the TodaiWW3-NK with higher spatial resolution produced higher H_s than that of IOWAGA. ERA5/ECWAM largely underestimates the wave height, despite its native spatial resolution of $0.36^o \times 0.36^o$, and assimilation of satellite altimeter data.

In summary, we have discovered that the exceedance probabilities of H_s derived from TodaiWW3-NK and satellite-altimeter agree quite well up to 19 m or so. However, their collocated comparison starts to deteriorate beyond 15 m. The disagreement is partly because we rarely observe extreme wave events over 15 m. In the following, we will study in-depth the selected historical extreme events.

3.2 Extreme event in January 2014

The North Atlantic Ocean experienced several distinct 10-year return period storms during the 2013-2014 winter (Castelle et al., 2015), but the storm that formed during January 4-6 was extraordinary. Hércules was an unprecedented storm covering almost the entire North Atlantic Ocean (Ponce De León & Guedes Soares, 2015b). By definition, Hércules is an explosive cyclone (Sanders & Gyakum, 1980), as the SLP dropped 38 hPa within 24 h; from 971 hPa at 00:00 UTC 04 Jan to 933 hPa, according to NOAA OPC synoptic maps (Figure S5 a,c). Extraordinary large swells reached the Iberian Peninsula causing devastating damage to the coastal region in France (Castelle et al., 2015) and in Portugal (Silva et al., 2017).

The spatial distribution of H_s at 2014.1.5 06:00 UTC from TodaiWW3-NK is shown in Figure 2a. The maximum significant wave height ($H_{s,max} = 21.26$ m) is attained at the south of the minimum SLP point and west of the warm front (Figure 2b), consistent with the depiction of the explosive cyclones in the Pacific Ocean (Kita et al., 2018). The area with high wave height also corresponds to where the directional spectrum narrows.

This extraordinary event in January 2014 exhibited a remarkable effect on the 25-year wave statistics. The comparison of the exceedance probabilities of H_s with and without the 2014.1 data revealed that this single event significantly enhanced the tail of the distribution (Figure 1b). When the 2014.1 data were excluded from the analysis, the largest H_s did not exceed 20.0 m. This means that the waves over 20 m H_s were associated only with the storm on January 4-6, 2014. We have also examined 25-year statistics from ERA5/ECMWF and IOWAGA/IFREMER, and both models unequivocally showed that the tail was enhanced by the January 2014 event (Figure S6).

Unquestionably, waves under Hércules is imperative in determining the 25-year North Atlantic wave statistics. However, it turns out that none of the satellite altimeters captured this event. JASON-2 is not an exception and missed the centre of the storm (Figure 2a). The highest H_s from the three models are 21.26 m, 20.43 m and 20.33 m from TodaiWW3-NK, IOWAGA, ERA5, respectively (Figures S7 a,c,e). However, even the JASON-2 track closest to the center largely underestimate the peak wave height under Hércules (Figures S7 b,d,f).

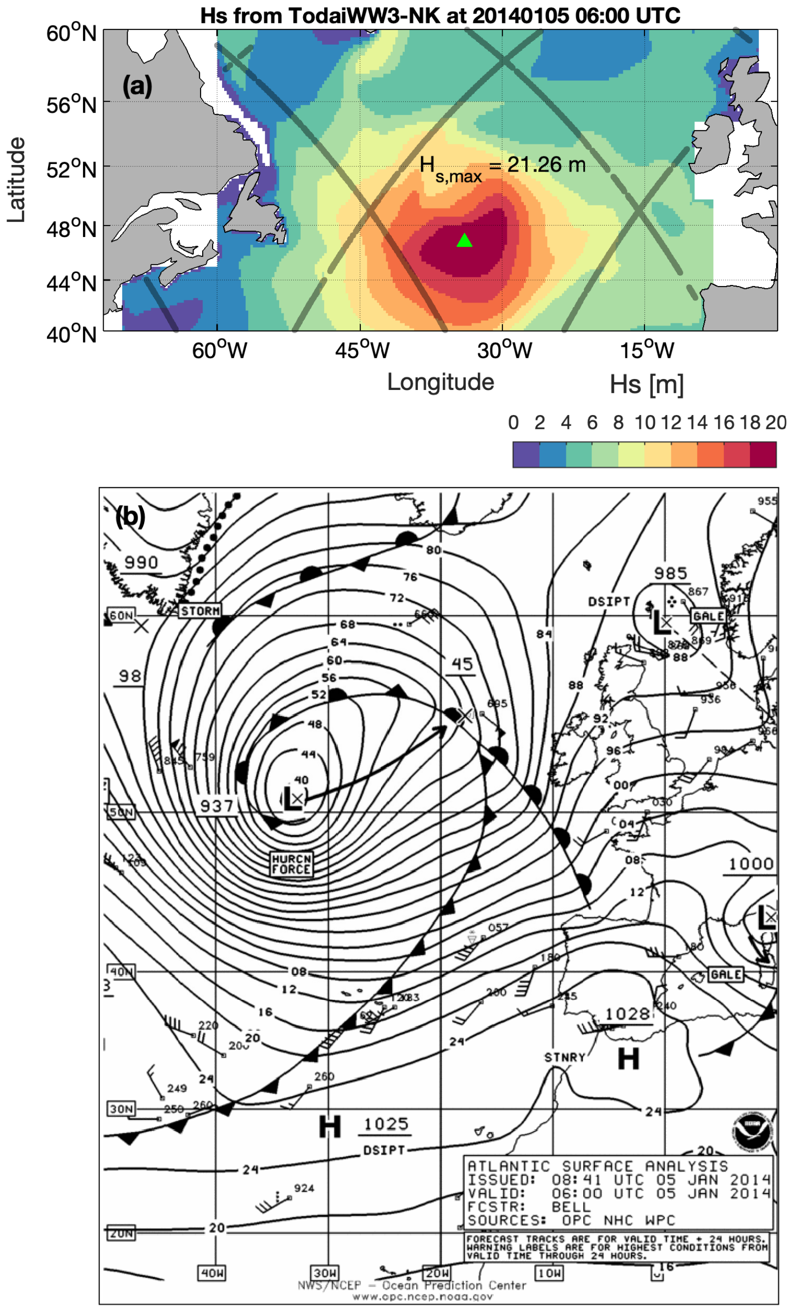

Figure 2. Spatial distribution of H_s from TodaiWW3-NK during the extreme event in January 2014. In subplot (a) the snapshot of H_s is shown for January 5, 2014 at 0600 UTC. The location of $H_{s,max}$ is highlighted by a green color triangle. The altimeter tracks of JASON-2 on January 5, 2014 are plotted on top of H_s. In subplot (b) NOAA OPC synoptic analysis charts is shown for 06:00 UTC on 05 Jan 2014.

The highest H_s from JASON-2 only went up to 15.5 m. We have scanned all the tracks of satellite altimeters that were operating during January 2014 and found that a segment of SARAL altimeter track passed closest to the center of the storm; the highest observed significant wave height reached $H_s = 19.24m$ at 48.20N, 29.42W, 20140105 07:23:22 UTC (Figures S7 g). Wave heights along this track were compared against the three independent hindcasts (Figures S7 h); both TodaiWW3-NK and IOWAGA seems to compare well with the altimeter derived data with a small bias, while ERA5 deviated by about 4 m at the storm peak and a large overall bias of -1.79 m (Table S1).

Satellites likely miss detecting the extreme waves under storms, and indeed the extreme waves under Hércules were not detected. As a consequence, removal of the 2014 data had hardly any effect on the satellite-derived 25-year exceedance probability. Then, why did the 25-year satellite-derived statistics compare well with the model (Figure 1a)?. Historical storms in the north Atlantic were identified and their impacts on the 25-year statistics were investigated. It turns out that the 2007 and 2011 storms contributed the most to enhance the tail of the satellite-derived distribution. By removing the two years from the statistics, the tail of the distribution reduced beyond 15 m, and underestimated the extremes compared to the full dataset (Figure 1c). Noting that these two storms were not as influential as the 2014 storm, this result suggests that the satellite-derived extreme wave heights are erroneous. To that end, we will compare models to satellites with available collocated buoy observations for the 2007 and 2011 events in section 3.3.

Lastly, the biases of the wave models may originate from the wind. We compared the CFSv2 wind speed that was used to force TodaiWW3-NK with the satellite wind data (Figures S8-S10). The maximum wind speeds were 47.4 ms^{-1}, 50.0 ms^{-1}, and 39.6 ms^{-1} for ASCAT, WindSat2, and OceanSat2, respectively, and were mostly faster than the maximum wind speed from CFSv2, 41.2 ms^{-1}. Therefore, it is unlikely that the model overestimated the 2014 event. Satellite-based measurements are known to have errors at high wind speeds (Hanafin et al., 2012).

3.3 Comparison of wave hindcasts with 2007 and 2011 extreme events

Both model and satellite observations need validation of the extremes. This is the lesson from the comparison of models and satellite observations of the January 2014 event. Here we analyze satellite altimeter data during the 2007 and 2011 extreme events when the JASON tracks were close to the storm center and registered H_s exceeding 20.0 m. The JASON-1 altimeter measured H_s=20.0 m during 9th February 2007 and the JASON-2 measured H_s=20.1 m on 14 February 2011 during the storm Quirin (Figures 3a,b). The H_s from TodaiWW3-NK, IOWAGA, and ERA5 are compared with the altimeter data (Figures 3c,d). The ERA5 consistently shows the lowest wave height while the TodaiWW3-NK shows the highest (Figures 3c,d). In the case of 2007 event, TodaiWW3-NK and IOWAGA compared well with the satellite, and in the case of 2011 event, IOWAGA tended to show lower wave heights than TodaiWW3-NK. Overall, TodaiWW3-NK reproduced the H_s well except at the peak of the event. This is attributed to the higher spatial resolution $0.20^{o} \times 0.25^{o}$ (Latitude $\times$ Longitude) of TodaiWW3-NK compared to IOWAGA and ERA5. Results from these analyses indicate that higher spatial resolution of the model plays an important role to capture wave heights during an extreme event.

Previous studies of the extreme events in 2007 and 2011 showed that the model reproduced high waves up to H_s=20.0 m, but provided that the wind forcing was tuned (Cardone et al., 2009; Ardhuin et al., 2011; Hanafin et al., 2012; Ponce De León & Guedes Soares, 2015a, 2015b). For the storm in February 2007, a WAM model simulation forced by CFSR wind agreed well with the JASON-1 along-track data, although the model slightly overestimated the H_s at the peak (Ponce de León & Guedes Soares, 2014). For the extreme event in February 2011, when the NCEP wind speed was increased by 10 %, the modeled H_s showed good agreement with JASON-2 along-track data (Ardhuin et al., 2011; Hanafin et

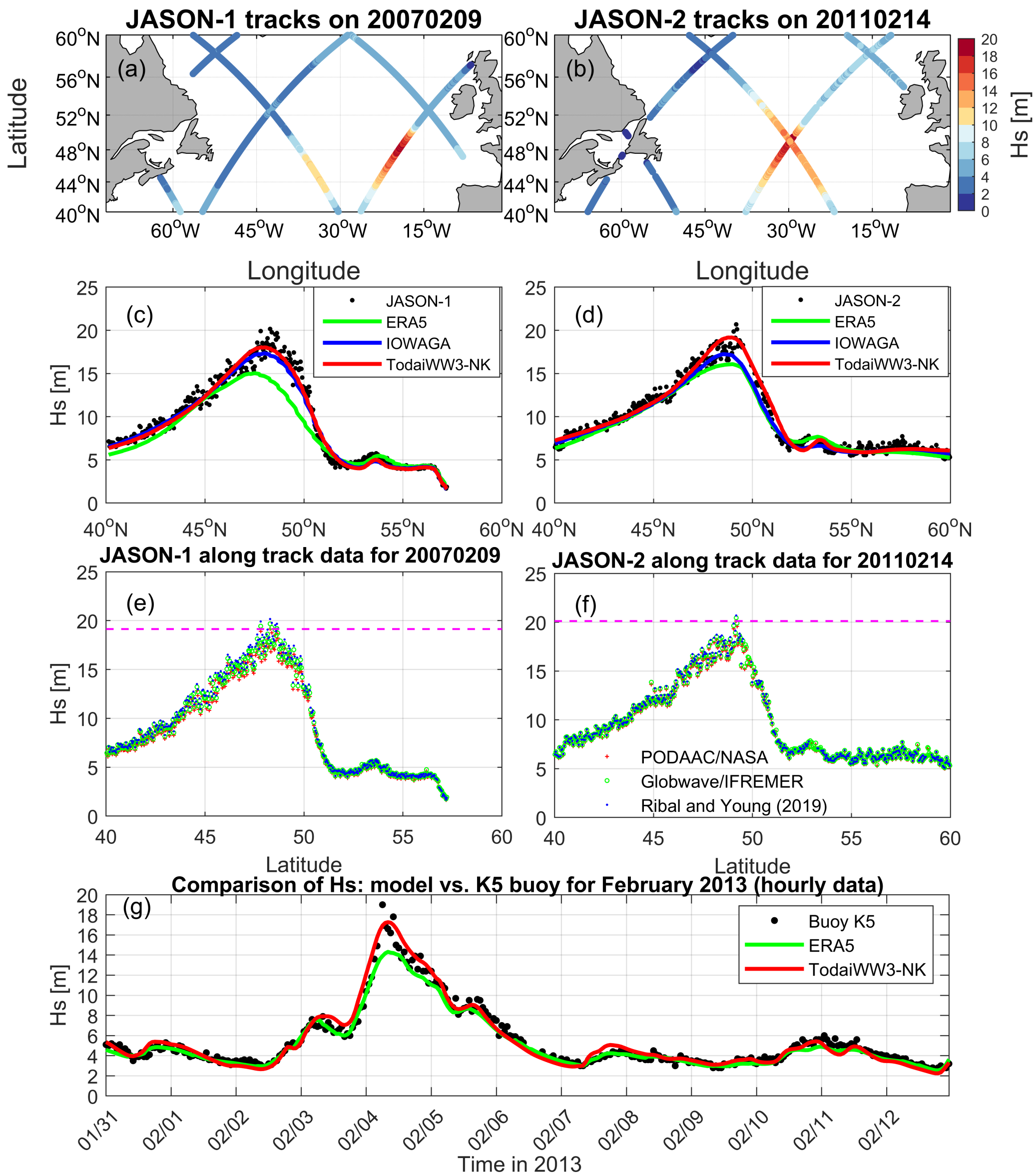

Figure 3. Significant wave height along JASON-1 tracks on February 9th 2007 and JASON-2 tracks on February 14th 2011 are shown in (a) and (b). Comparison of models against altimeter along track data are shown in subplots (c) and (d). Satellite altimeter products from PODAAC/NASA, Globwave/IFREMER, and Ribal and Young (2019), are compared for: (e) the extreme event on February 9, 2007, from the JASON-1; (f) the extreme event on February 14, 2011, from the JASON-2. In subplot (g), a comparison of significant wave heights between models and buoy observations are presented for the extreme event in February 2013. The time-series of hourly H_s data from UK Met Office buoy K5 and models are compared. The IOWAGA data is not included in this comparison as it is 3-hourly data.

al., 2012). Whereas, in TodaiWW3-NK, the value of wind-wave growth parameter of the ST4 model physics was tuned to $\beta_{max} = 1.33$ (CFSR wind forcing), which is consistent with IOWAGA.

However, validating the model against one satellite product is not the end of the story. It turns out that different satellite H_s products produce a large deviation in their estimates. For these two extreme events, we compared different JASON-1 and JASON-2 altimeter products obtained from Ribal and Young (2019) (RY), Globwave (GW), and PODAAC/NASA (PN) (Figure 3e,f). For H_s <10 m, altimeter products compare well, however for H_s beyond 10-12 m, the altimeter products start to scatter as much as a few meters and deviate among them. For the extreme event in February 2007, the maximum H_s from RY, GW, and PN are 20.16 m, 19.67 m, and 19.13 m, respectively. Whereas during the extreme event in February 2011, the maximum H_s from RY, GW, and PN are 20.69 m, 20.44 m, and 20.12 m, respectively. Overall, H_s from RY was the largest, and H_s from PN was the smallest, with a bias of around 0.4 m. Despite derived from identical satellite altimeter, the H_s from different sources show deviation because the algorithm used to derive them are different. Finally, we conjecture that the bias and the large intermittency of the satellite-derived H_s may have contributed to the overestimation of the 2007 and 2011 extreme events. As a result, the tail of the exceedance probability was erroneously enhanced (Figure 1c).

3.4 The highest H_s as measured by a buoy in 2013

Finally, this section illustrates the significance of in-situ observation. None of the extreme events in 2007, 2011, and 2014 studied in this paper were registered by in-situ observations. Historically, no buoys had observed waves higher than 20 m. The largest wave height registered by a buoy is 19.0 m from the UK Met Office (K5 buoy) during an extreme event in Feb 2013. The record was examined by the World Meteorological Organization expert committee and was reported as "the highest significant wave height as measured by a buoy." Here we present a comparison of the buoy observation with hourly data from ERA5 and TodaiWW3-NK (Figure 3g). As aforementioned, ERA5 underestimates the extreme, whereas TodaiWW3-NK mostly follows the rapid increase of H_s. We also note a spiky nature of the buoy estimated H_s; the 19 m H_s rapidly drops to around 17 m or less for the following 3 hours, and then increases again to 18 m or so, immediately followed by a drop to 15 m or less. We may attribute such intermittency of the in-situ observation to the sampling variability or by the intrinsic variability not resolved by the model (Bitner-Gregersen & Magnusson, 2014). Besides, the accelerometer-based buoy observation may require special attention in detecting extremes (Collins et al., 2014). As such, the in-situ data itself needs to be validated at the extreme event. More in-situ observations are necessary.

4 Summary and Conclusions

In this paper we have revisited the wave statistics of the GWS 8,9,15,16 areas in the North Atlantic Ocean by analyzing 25 years of hindcast and reanalysis wave data from ERA5, IOWAGA, and TodaiWW3-NK. The TodaiWW3-NK based exceedance probability of H_s compared well with altimeter-derived data up to almost 20.0 m. Within the 25 years (1994-2018), the maximum value of H_s exceeded 21.0 m from TodaiWW3-NK during the storm Hercules in January 4-6, 2014. The impact of this single storm on 25-year wave statistics is noteworthy as it significantly enhanced the tail of H_s distribution. The comparison of H_s between models and altimeter data for three extreme events reveal that the tail of the distribution was most enhanced with TodaiWW3-NK, slightly less enhanced with IOWAGA and largely reduced with ERA5. The difference of the first two is attributed to the difference in their spatial resolutions.

The finding that the H_s at the peak of the 2014 storm was not detected by JASON-2 was unanticipated and suggests that the 25-year altimeter derived statistics is independent of this event. Since the three independent models unequivocally demonstrated the anomalous impact of the 2014 storm, we then conjectured that the extreme waves detected by satellite altimeter have large uncertainty. Moreover, for the extreme wave heights, the JASON-2 derived H_s products largely differed among the estimates (PODAAC/NASA, Globwave/IFREMER, Ribal and Young, 2019). Besides, altimeters have their limitation in providing a spatial coverage as the H_s is measured along the tracks only. Therefore, the extreme events may not be fully detected by altimeters due to under-sampling. To achieve a better spatial coverage of H_s during an extreme event such as a storm, altimeters with higher sampling will be useful (i.e., repeat cycle less than 10 days). The satellite altimeter data have never been calibrated for the extremes, and we expect that the cross calibration of H_s (e.g. Ribal and Young 2019) will be performed for H_s beyond 10 m in the future.

In-situ wave measurements during extreme events are essential for the calibration of altimeter data and validation of model results. However, there are no in-situ wave measurements available in the open water of the North Atlantic Ocean. In the past, the moored buoy network of UK Met Office measured H_s up to 18.0-19.0 m, although these buoys are not under the area of historical extreme wave events. More in-situ wave measurements are required in the open ocean during extreme events. Recently, the spotter buoy network in the Pacific Ocean started to provide valuable wave information with more than 150 spotter buoys. However, until now, there is no such buoy network in the North Atlantic Ocean. Therefore, a network of similar buoys in the North Atlantic Ocean, if deployed, will provide us a better insight of H_s during extreme events in the future.

Acknowledgments
The study presented in this paper was carried out within a joint research project between the University of Tokyo and Nippon Kaiji Kyokai (ClassNK).
ERA5 data is available on the Copernicus Climate Change Service (C3S) Climate Data Store, and IOWAGA data is available from the IOWAGA-Ifremer data base. Their URLs are listed in the Supporting Information together with links to Ribal and Young (2019) data, Globwave altimeter data, PODAAC/NASA altimeter data, buoy data, Satellite winds (Widsat, ASCAT, OceanSat-2) and CFSR wind and sea ice concentration.

References

Alves, J. H. G., & Young, I. R. (2003). On estimating extreme wave heights using combined geosat, topex/poseidon and ers-1 altimeter data. *Applied Ocean Research*, *25*(4), 167–186.

Ardhuin, F., Hanafin, J., Quilfen, Y., Chapron, B., Queffeulou, P., Obrebski, M., … Vandemark, D. (2011). Calibration of the iowaga global wave hindcast (1991–2011) using ecmwf and cfsr winds. In *Proceedings of the 2011 international workshop on wave hindcasting and forecasting and 3rd coastal hazard symposium, kona, hi, usa* (Vol. 30).

Ardhuin, F., Rogers, E., Babanin, A. V., Filipot, J.-F., Magne, R., Roland, A., … others (2010). Semiempirical dissipation source functions for ocean waves. part i: Definition, calibration, and validation. *Journal of Physical Oceanography*, *40*(9), 1917–1941.

Bitner-Gregersen, E. M., Dong, S., Fu, T., Ma, N., Maisondieu, C., Miyake, R., & Rychlik, I. (2016). Sea state conditions for marine structures' analysis and model tests. *Ocean Engineering*, *119*, 309–322.

Bitner-Gregersen, E. M., & Magnusson, A. K. (2014). Effect of intrinsic and sampling variability on wave parameters and wave statistics. *Ocean Dynamics*, *64*(11), 1643–1655.

Cardone, V., Callahan, B., Chen, H., Cox, A., Morrone, M., & Swail, V. (2015). Global distribution and risk to shipping of very extreme sea states (vess). *International Journal of Climatology*, *35*(1), 69–84.

Cardone, V., Cox, A., Morrone, M., & Swail, V. R. (2009). Satellite altimeter detection of global very extreme sea states (vess). In *Proc. 11th int. workshop on wave hindcasting and forecasting.*

Cardone, V., Cox, A. T., Morrone, M. A., & Swail, V. R. (2011). Global distribution and associated synoptic climatology of very extreme sea states (vess). In *Proceedings 12th international workshop on wave hindcasting and forecasting, hawaii.*

Castelle, B., Marieu, V., Bujan, S., Splinter, K. D., Robinet, A., Sénéchal, N., & Ferreira, S. (2015). Impact of the winter 2013–2014 series of severe western europe storms on a double-barred sandy coast: Beach and dune erosion and megacusp embayments. *Geomorphology*, *238*, 135–148.

Collins, C. O., Lund, B., Waseda, T., & Graber, H. C. (2014). On recording sea surface elevation with accelerometer buoys: lessons from itop (2010). *Ocean Dynamics*, *64*(6), 895–904.

Hanafin, J. A., Quilfen, Y., Ardhuin, F., Sienkiewicz, J., Queffeulou, P., Obrebski, M., … others (2012). Phenomenal sea states and swell from a north atlantic storm in february 2011: a comprehensive analysis. *Bulletin of the American Meteorological Society*, *93*(12), 1825–1832.

Hersbach, H., Bell, B., Berrisford, P., Hirahara, S., Horányi, A., Muñoz-Sabater, J., … others (2020). The era5 global reanalysis. *Quarterly Journal of the Royal Meteorological Society*.

Hogben, N., Da Cunha, L., & Oliver, H. (1986). Global Wave Statistics. *Unwin Brothers Limited London, England*.

IACS. (2001). International association of classification societies. Recommendation no. 34, standard wave data. http://www.iacs.org.uk.

Kita, Y., Waseda, T., & Webb, A. (2018). Development of waves under explosive cyclones in the northwestern pacific. *Ocean Dynamics*, *68*(10), 1403–1418.

Ponce de León, S., Bettencourt, J. H., Brennan, J., & Dias, F. (2015). Evolution of the extreme wave region in the north atlantic using a 23 year hindcast. In *International conference on offshore mechanics and arctic engineering* (Vol. 56499, p. V003T02A019).

Ponce de León, S., & Guedes Soares, C. (2014). Extreme wave parameters under north atlantic extratropical cyclones. *Ocean Modelling*, *81*, 78–88.

Ponce De León, S., & Guedes Soares, C. (2015a). Hindcast of extreme sea states in north atlantic extratropical storms. *Ocean Dynamics*, *65*(2), 241–254.

Ponce De León, S., & Guedes Soares, C. (2015b). Hindcast of the hércules winter storm in the north atlantic. *Natural Hazards*, *78*(3), 1883–1897.

Rascle, N., & Ardhuin, F. (2013). A global wave parameter database for geophysical applications. part 2: Model validation with improved source term parameterization. *Ocean Modelling*, *70*, 174–188.

Ribal, A., & Young, I. R. (2019). 33 years of globally calibrated wave height and wind speed data based on altimeter observations. *Scientific data*, *6*(1), 1–15.

Saha, S., Moorthi, S., Pan, H.-L., Wu, X., Wang, J., Nadiga, S., … others (2010). The NCEP climate forecast system reanalysis. *Bulletin of the American Meteorological Society*, *91*(8), 1015–1058.

Saha, S., Moorthi, S., Wu, X., Wang, J., Nadiga, S., Tripp, P., … others (2014). The NCEP climate forecast system version 2. *Journal of Climate*, *27*(6), 2185–2208.

Sanders, F., & Gyakum, J. R. (1980). Synoptic-dynamic climatology of the bomb. *Monthly Weather Review*, *108*(10), 1589–1606.

Silva, S. F., Martinho, M., Capitão, R., Reis, T., Fortes, C. J., & Ferreira, J. C. (2017). An index-based method for coastal-flood risk assessment in low-lying areas (costa de caparica, portugal). *Ocean & Coastal Management*, *144*, 90–104.

Turton, J., & Fenna, P. (2008). Observations of extreme wave conditions in the north-east atlantic during december 2007. *Weather*, *63*(12), 352–355.

Figure 1.

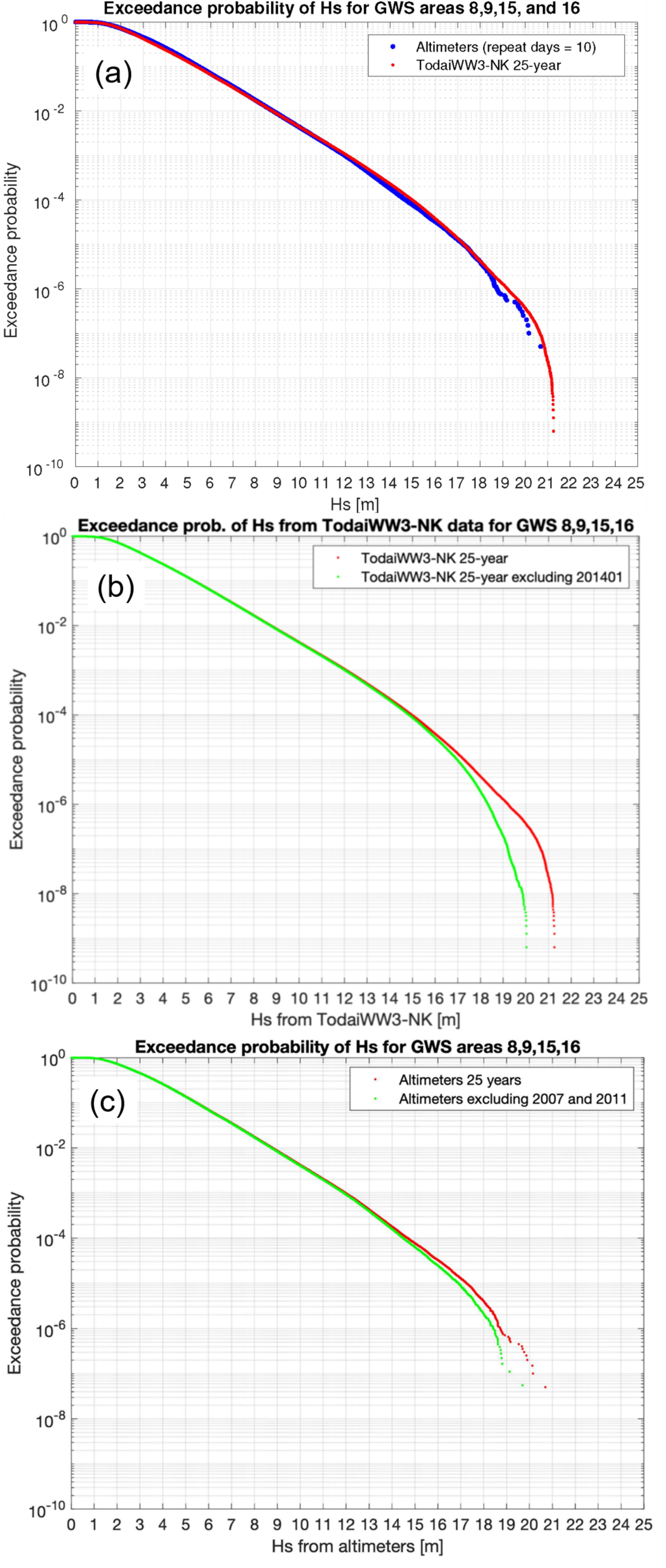

Exceedance probability of Hs for GWS areas 8,9,15, and 16
(a)
Altimeters (repeat days = 10)
TodaiWW3-NK 25-year
Exceedance probability
Hs [m]
Exceedance prob. of Hs from TodaiWW3-NK data for GWS 8,9,15,16
(b)
TodaiWW3-NK 25-year
TodaiWW3-NK 25-year excluding 201401
Exceedance probability
Hs from TodaiWW3-NK [m]
Exceedance probability of Hs for GWS areas 8,9,15,16
(c)
Altimeters 25 years
Altimeters excluding 2007 and 2011
Exceedance probability
Hs from altimeters [m]

Figure 2.

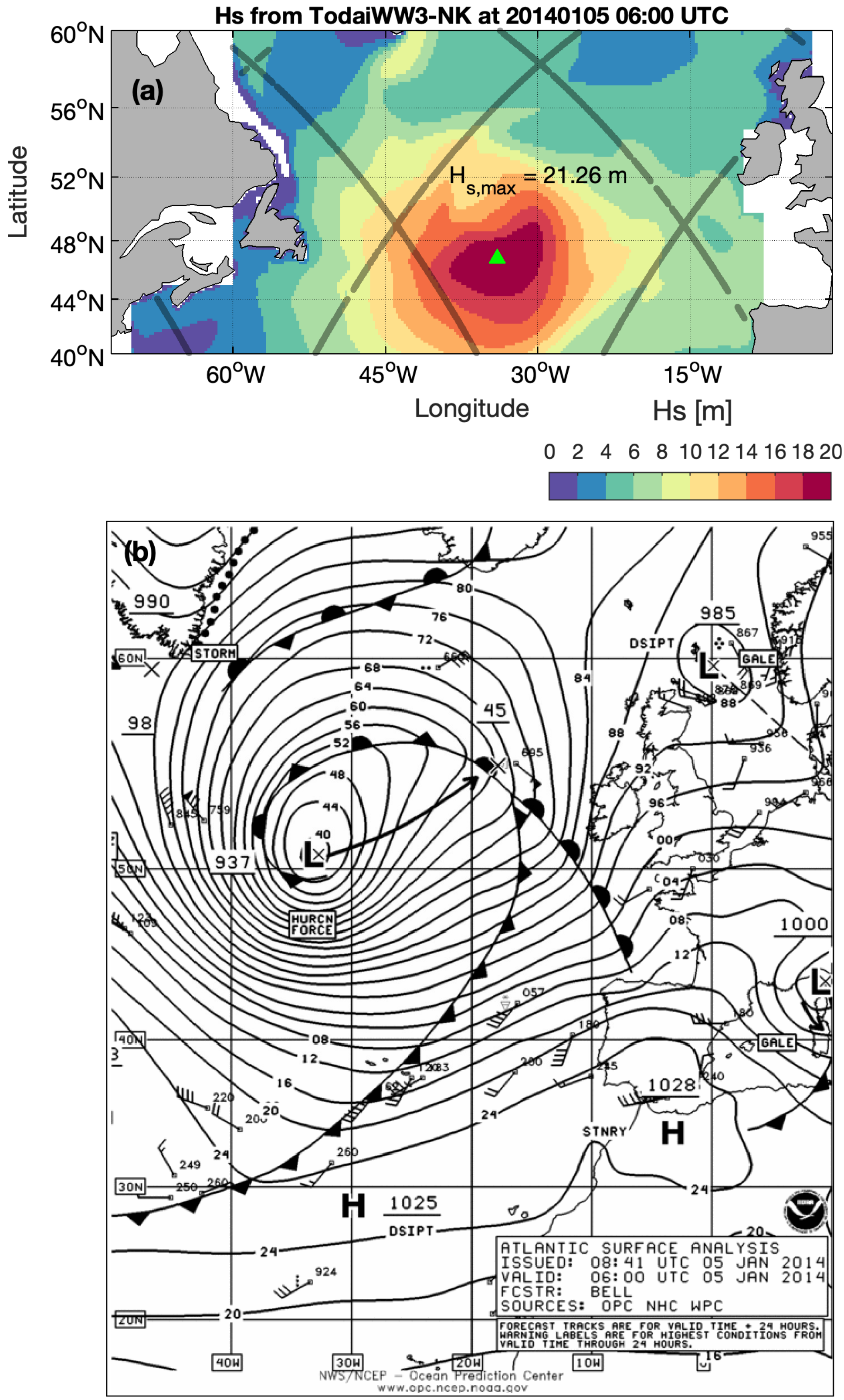
Hs from TodaiWW3-NK at 20140105 06:00 UTC
(a)
$H_{s,max}$ = 21.26 m
60°N
56°N
52°N
48°N
44°N
40°N
Latitude
60°W
45°W
30°W
15°W
Longitude
Hs [m]
0 2 4 6 8 10 12 14 16 18 20
(b)
990
STORM
98
937
HURCN FORCE
985
DSIPT
GALE
45
1000
1028
STNRY
H
1025
DSIPT
ATLANTIC SURFACE ANALYSIS
ISSUED: 08:41 UTC 05 JAN 2014
VALID: 06:00 UTC 05 JAN 2014
FCSTR: BELL
SOURCES: OPC NHC WPC
FORECAST TRACKS ARE FOR VALID TIME + 24 HOURS.
WARNING LABELS ARE FOR HIGHEST CONDITIONS FROM
VALID TIME THROUGH 24 HOURS.
60N
50N
40N
30N
20N
40W
30W
20W
10W
NWS/NCEP - Ocean Prediction Center
www.opc.ncep.noaa.gov

Figure 3.

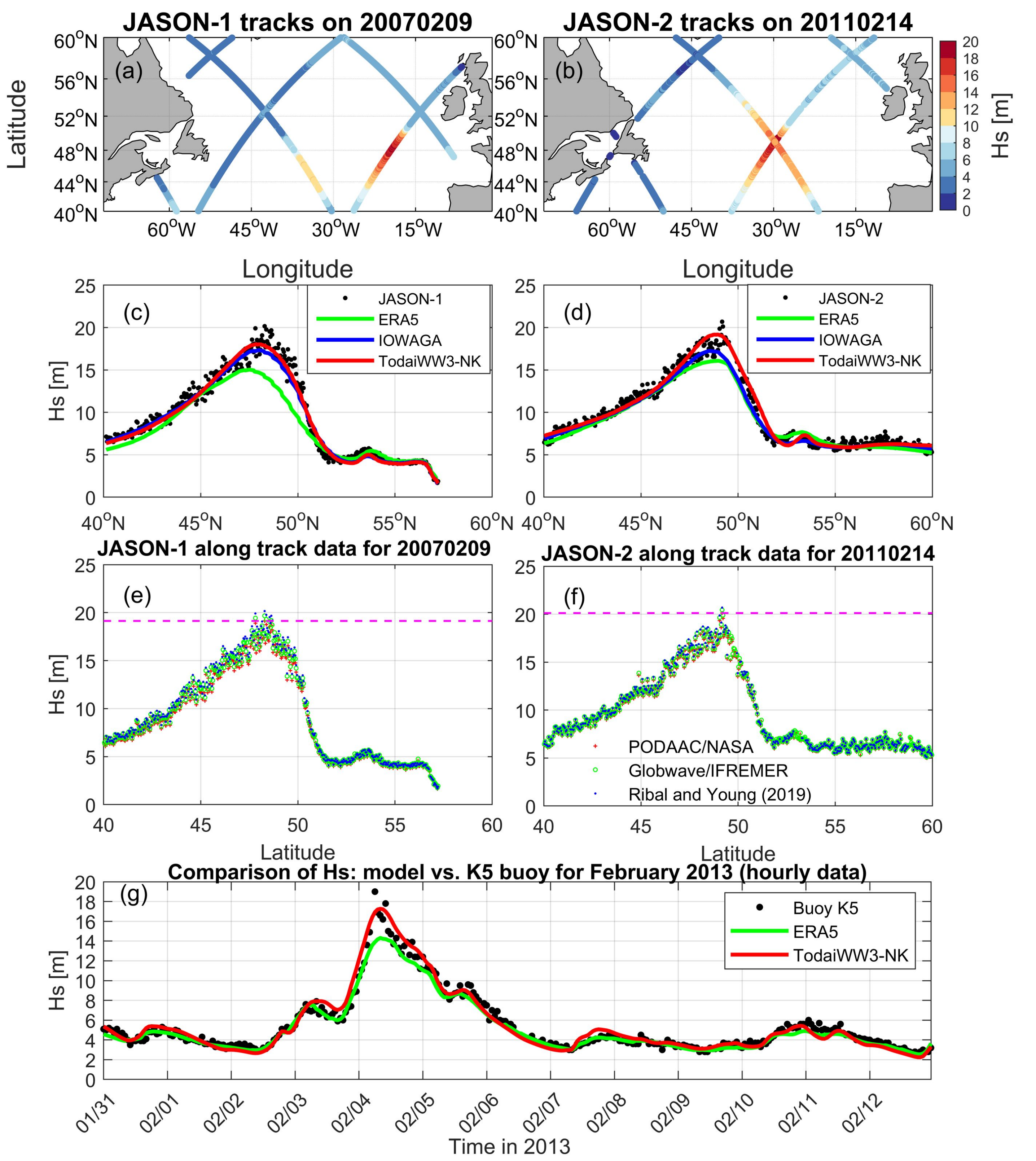

JASON-1 tracks on 20070209
JASON-2 tracks on 20110214
(a)
(b)
Latitude
Longitude
Hs [m]
60°N
56°N
52°N
48°N
44°N
40°N
60°W
45°W
30°W
15°W
(c)
(d)
JASON-1
JASON-2
ERA5
IOWAGA
TodaiWW3-NK
JASON-1 along track data for 20070209
JASON-2 along track data for 20110214
(e)
(f)
PODAAC/NASA
Globwave/IFREMER
Ribal and Young (2019)
Latitude
Comparison of Hs: model vs. K5 buoy for February 2013 (hourly data)
(g)
Buoy K5
ERA5
TodaiWW3-NK
Time in 2013

Supporting Information for "Modeled and satellite-derived extreme wave height statistics in the North Atlantic Ocean reaching 20 m"

Kaushik Sasmal[1], Tsubasa Kodaira[1], Yuki Kita[2], Rei Miratsu[3], Tingyao Zhu[3], Tsutomu Fukui[3], Takuji Waseda[1]

[1]Graduate School of Frontier Sciences, The University of Tokyo, Kashiwa, Chiba, Japan

[2]MS & AD InterRisk Research & Consulting, Inc., Chiyoda, Tokyo, Japan

[3]Nippon Kaiji Kyokai (ClassNK), Chiyoda, Tokyo, Japan

Contents of this file

Text S1.

1. Model Set-up

TodaiWW3-NK is based on third–generation spectral wave model NOAA WAVEWATCH III version 6.07 (The WAVEWATCH III® Development Group (WW3DG), 2019). The model computational domain encompasses the Atlantic Ocean. The bathymetry data for the model was derived from ETOPO1 (Amante & Eakins, 2009). The spatial resolution of the model is $0.20^{o} \times 0.25^{o}$ (Lat $\times$ Lon). There are 35 frequency bins and 36 directional bins. The lowest and the highest frequencies were set to 0.04118 Hz and 1.1 Hz. For model physics, the ST4 package of Ardhuin et al. (2010) was used. The model was forced by NCEP/CFSR hourly wind (Saha et al., 2010, 2014). NCEP/CFSR daily sea ice concentration was provided to the model as a source of sea ice. A one-month spin-up run was carried out and the model was integrated for 25 years in hindcast mode (1994-2018). Significant wave height (Hs) was post-processed from model output for GWS areas 8,9,15, and 16. The Hs from the model is validated against satellite altimeter data (Ribal & Young, 2019) and UK Met Office buoy data.

1.1. Equations for statistics

$$\mathrm{CC} = \frac{\sum_{i=1}^{n}(x_i - \bar{x})(y_i - \bar{y})}{\sqrt{\sum_{i=1}^{n}(x_i - \bar{x})^2}\sqrt{\sum_{i=1}^{n}(y_i - \bar{y})^2}}, \tag{1}$$

$$\mathrm{Bias} = \frac{1}{n}\sum_{i=1}^{n}(y_i - x_i), \tag{2}$$

$$\mathrm{RMSE} = \sqrt{\frac{1}{n}\sum_{i=1}^{n}(y_i - x_i)^2}, \tag{3}$$

$$\mathrm{SI} = \frac{RMSE}{\bar{x}}, \tag{4}$$

where x_i is the observed value, y_i is the computed value of wave parameter, n is the number of observations, $\bar{x}$ is the averaged observed value, $\bar{y}$ is the averaged computed value.

References

Amante, C., & Eakins, B. (2009). ETOPO1 1 arc-minute global relief model: procedures, data sources and analysis. NOAA technical memorandum NESDIS NGDC-24. *National Geophysical Data Center, NOAA.*

Ardhuin, F., Rogers, E., Babanin, A. V., Filipot, J.-F., Magne, R., Roland, A., ... others (2010). Semiempirical dissipation source functions for ocean waves. part i: Definition, calibration, and validation. *Journal of Physical Oceanography*, *40* (9), 1917–1941.

Hersbach, H., Bell, B., Berrisford, P., Hirahara, S., Horányi, A., Muñoz-Sabater, J., ... others (2020). The era5 global reanalysis. *Quarterly Journal of the Royal Meteorological Society*.

Rascle, N., & Ardhuin, F. (2013). A global wave parameter database for geophysical applications. part 2: Model validation with improved source term parameterization. *Ocean Modelling*, *70*, 174–188.

Ribal, A., & Young, I. R. (2019). 33 years of globally calibrated wave height and wind speed data based on altimeter observations. *Scientific data*, *6* (1), 1–15.

Saha, S., Moorthi, S., Pan, H.-L., Wu, X., Wang, J., Nadiga, S., ... others (2010). The NCEP climate forecast system reanalysis. *Bulletin of the American Meteorological Society*, *91* (8), 1015–1058.

Saha, S., Moorthi, S., Wu, X., Wang, J., Nadiga, S., Tripp, P., ... others (2014). The NCEP climate forecast system version 2. *Journal of Climate*, *27*(6), 2185–2208.

The WAVEWATCH III® Development Group (WW3DG). (2019). User manual and system documentation of WAVEWATCH III® version 6.07. *Tech. Note 333*, *NOAA/NWS/NCEP/MMAB, College Park, MD, USA, 465 pp. +Appendices.*.

Table S1. Comparison of H_s statistics between models and observations.

Extreme event Date and time	Model	Statistics CC	Bias (m)	RMSE (m)	SI
20140105 07:23:22 UTC	ERA5	0.97	-1.79	2.45	0.22
SARAL (Ka band)	IOWAGA	0.98	-0.02	0.98	0.09
	TodaiWW3-NK	0.98	0.18	0.93	0.08
20070209 21:30:40 UTC	ERA5	0.96	-1.05	1.95	0.21
JASON-1 (Ku C band)	IOWAGA	0.99	-0.25	0.85	0.09
	TodaiWW3-NK	0.99	-0.18	0.76	0.08
20110214 11:03:10 UTC	ERA5	0.98	-0.57	1.04	0.11
JASON-2 (Ku C band)	IOWAGA	0.99	-0.36	0.78	0.08
	TodaiWW3-NK	0.98	0.10	0.75	0.08
20130204 06:00:00 UTC	ERA5	0.99	-0.28	0.64	0.12
K5 buoy	TodaiWW3-NK	0.98	0.06	0.63	0.12

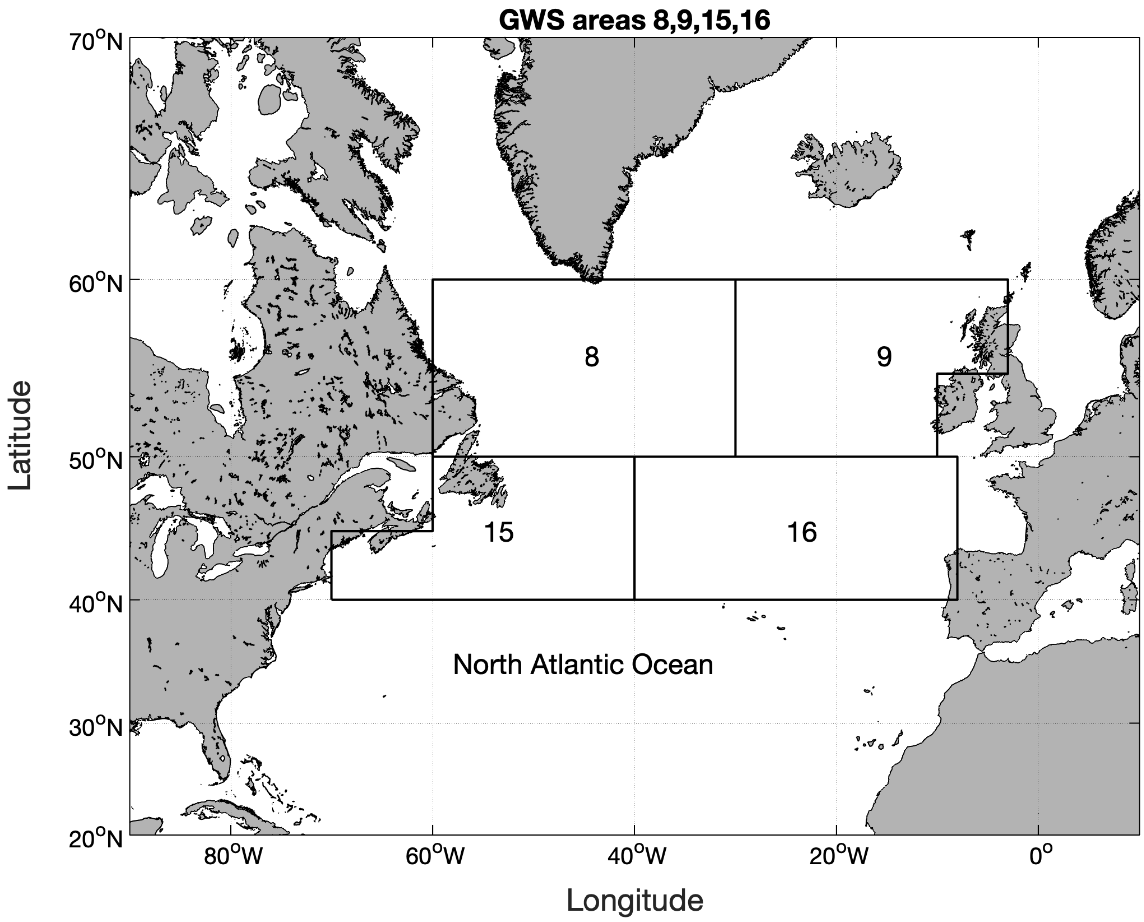

Figure S1. Map of study region and the Global Wave Statistics (GWS) areas 8,9,15,16 are shown.

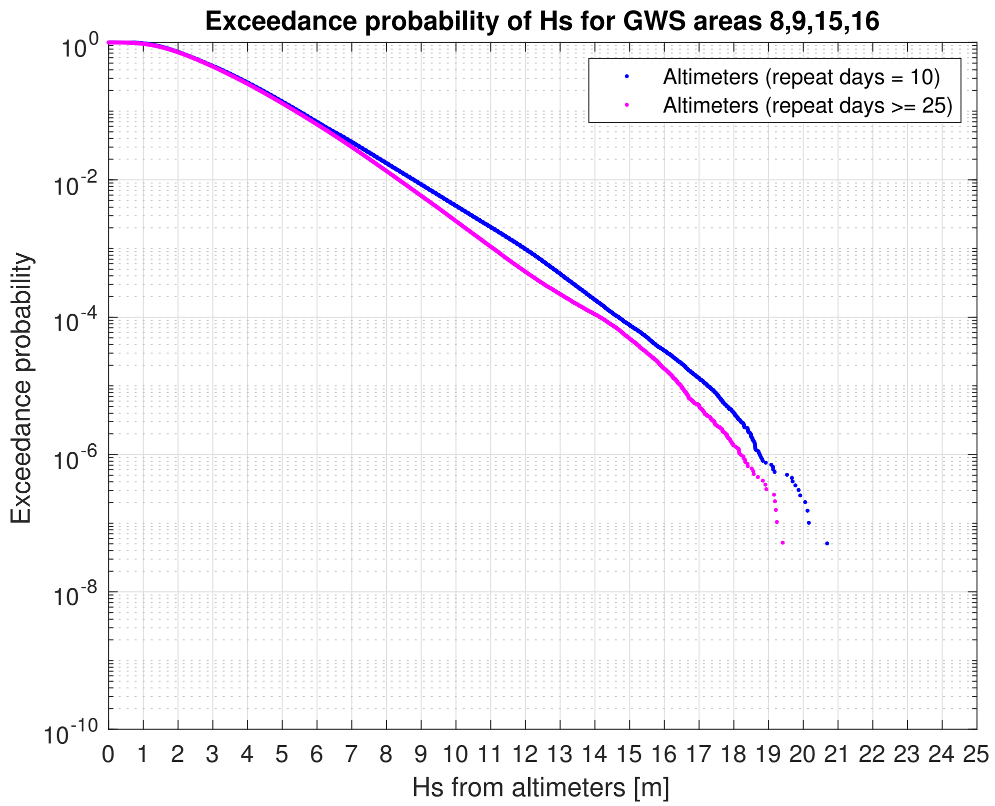

Figure S2. Comparison of exceedance probability of significant wave height between altimeters with repeat cycle=10 days and repeat cycle >=25 days. The altimeters with repeat cycle=10 days are TOPEX, JASON-1, JASON-2, and JASON-3. The altimeters with repeat cycle >=25 days are ERS-2, ENVISAT, CRYOSAT-2, SARAL, and SENTINEL-3A. The comparison is made for GWS areas 8,9,15 and 16 using 25 years data from 1994 to 2018.

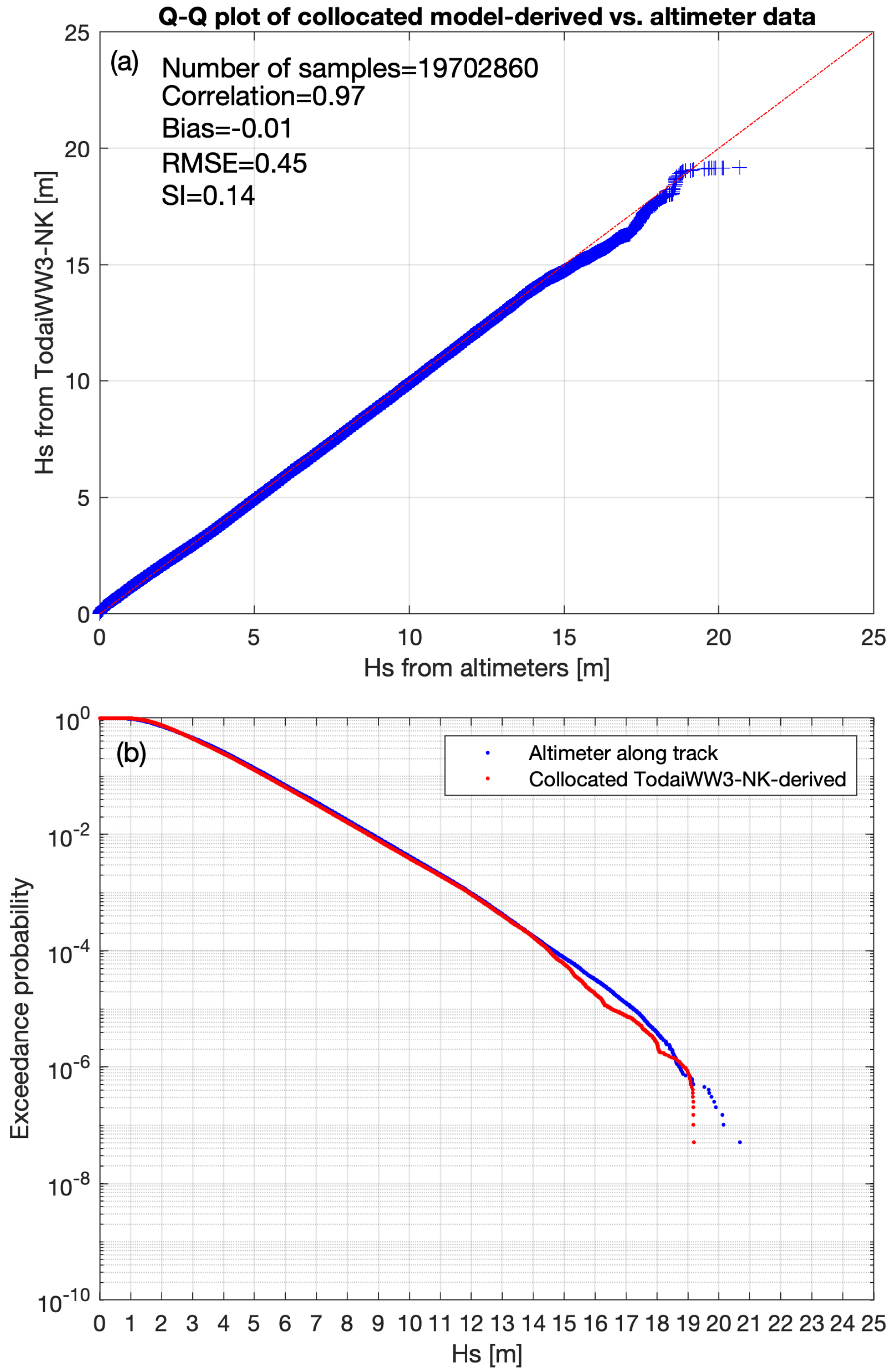

Figure S3. (a) Q-Q plot of Hs between TodaiWW3-NK and altimeter derived data for the GWS 8,9,15,16. (b) Comparison of exceedance probability of Hs between TodaiWW3-NK and altimeter derived data. Here the collocated model derived and altimeter along track derived data for 25 years from 1994-2018 are used for the comparson.

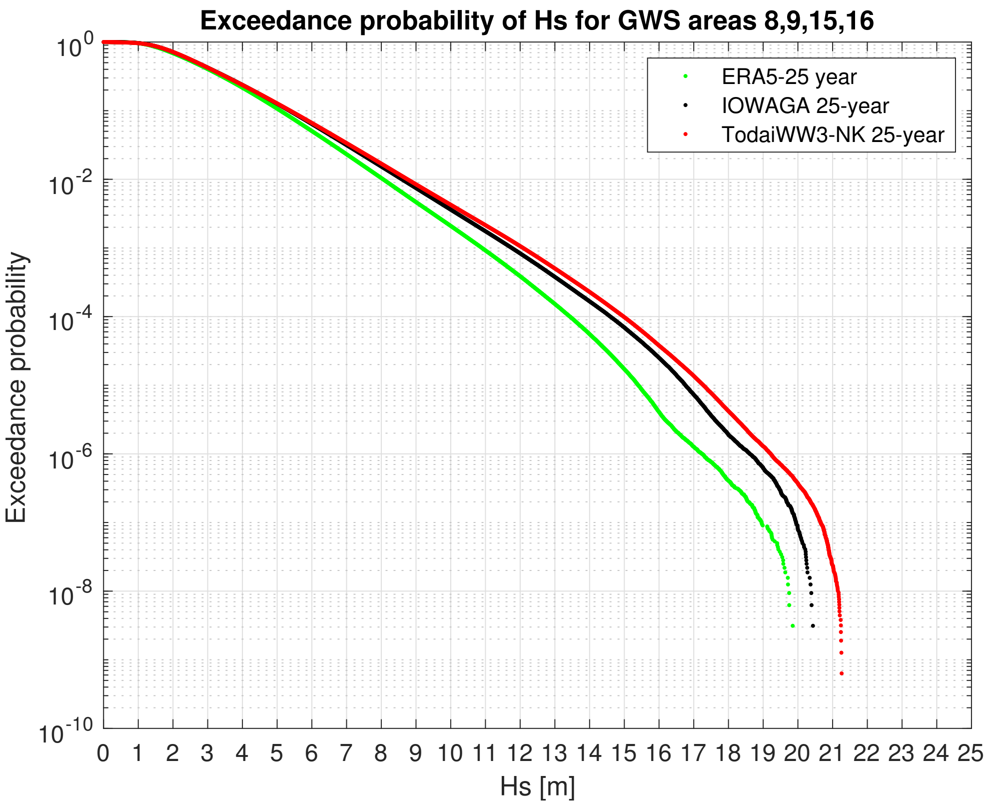

Figure S4. Comparison of exceedance probability of Hs between models for the GWS 8,9,15,16. Here 25 years of data from 1994-2018 are used.

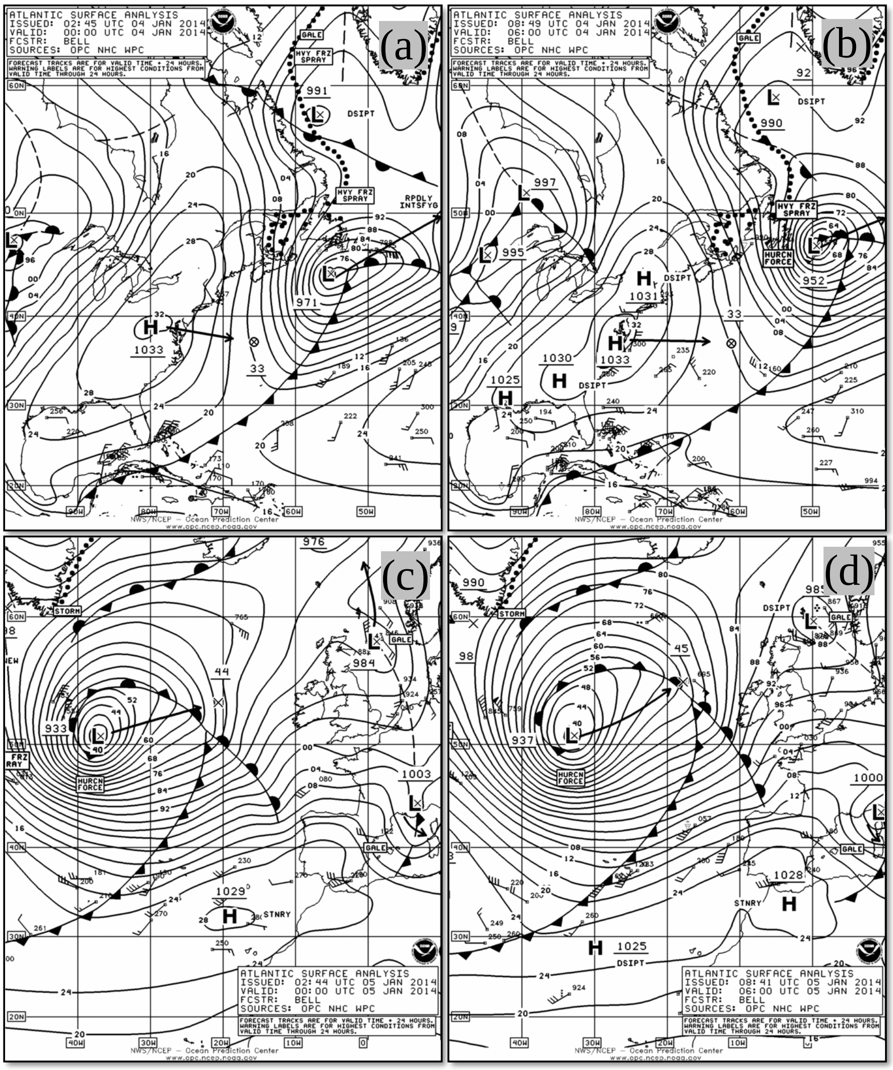

Figure S5. NOAA OPC synoptic analysis charts for 00:00 UTC and 06:00 UTC on 04 Jan 2014 (a,b) and for 00:00 UTC and 00:06 UTC on 05 Jan 2014 (c,d). On 04 Jan, the storm was near 44°N, 55°W with a SLP of 971 hPa at the center. It was expected to track northeast (shown by the arrow) and rapidly intensify to hurricane force. By 0000 UTC on 05 Jan, the storm had intensified with SLP of 933 hPa at the center of the storm with hurricane-force winds and moved to 51°N, 38°W.

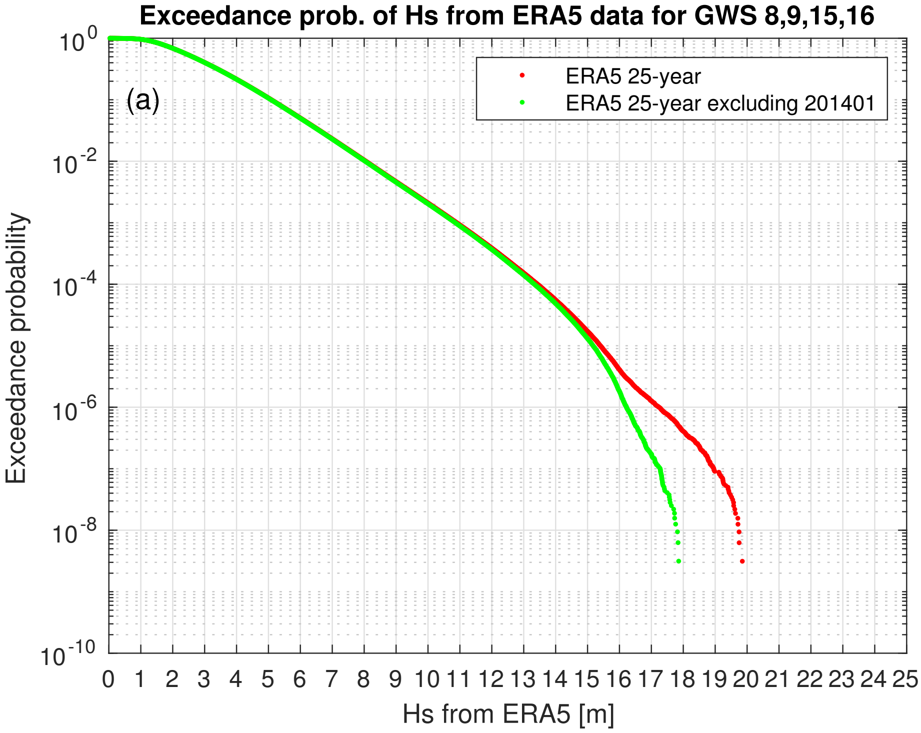

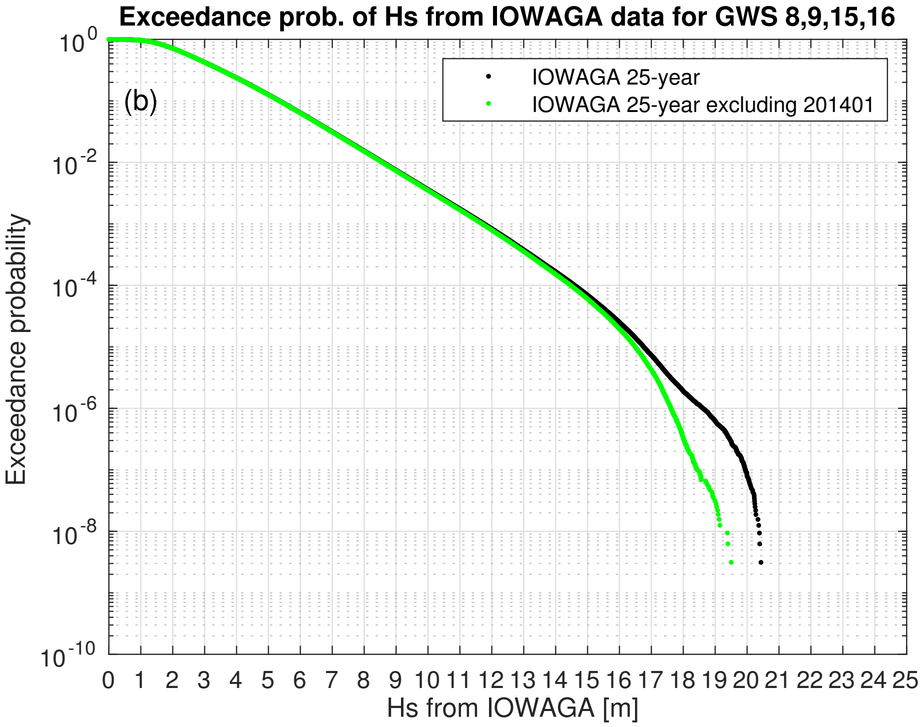

Figure S6. The exceedance probability of Hs is compared with and without January 2014 data. (a) Exceedance probability of significant wave height from ERA5 using 25 year 3-hourly data from 1994 to 2018 for GWS areas 8,9,15 and 16. (b) Exceedance probability of significant wave height from IOWAGA using 25 year 3-hourly data from 1994 to 2018 for GWS areas 8,9,15 and 16.

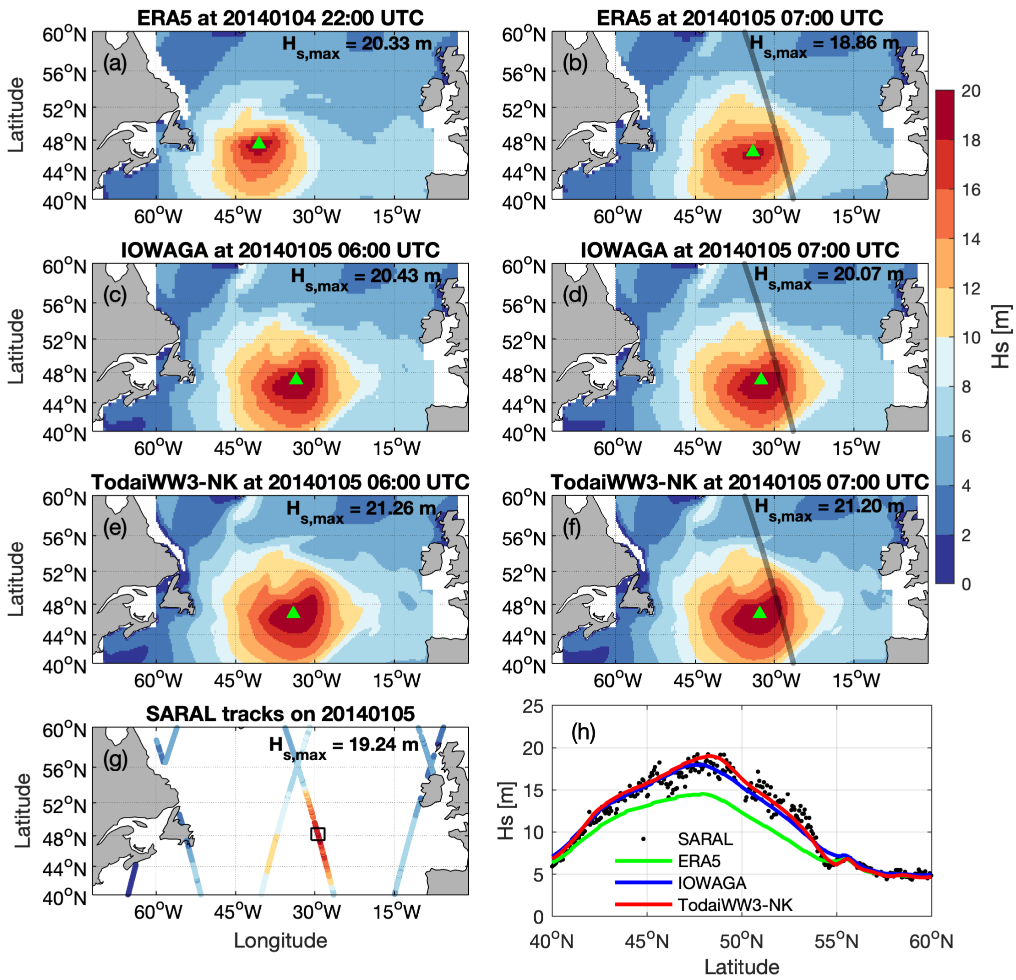

Figure S7. Spatial distribution of Hs from ERA5, IOWAGA and TodaiWW3-NK data during the extreme event in January 2014. The subplots (a) and (b) show the snapshots of Hs from ERA5 data. The subplots (c) and (d) show Hs from IOWAGA, and subplots (e) and (f) illustrate Hs from TodaiWW3-NK data. The Hs,max in the IOWAGA and TodaiWW3-NK dataset is found to occcur at 20140105 0600 UTC, whereas, Hs,max from ERA5 data is identified at 20140104 22:00 UTC. The values of the Hs,max are highlighted. Subplot (g) shows segments of altimeter tracks from SARAL on 20140105 and the rectangle in solid black line points to the location of Hs,max in the altimeter data. The subplot (h) shows a comparison of Hs between models and altimeter for a particular segment of the track shown in subplot (g) that passed close to the storm centre.

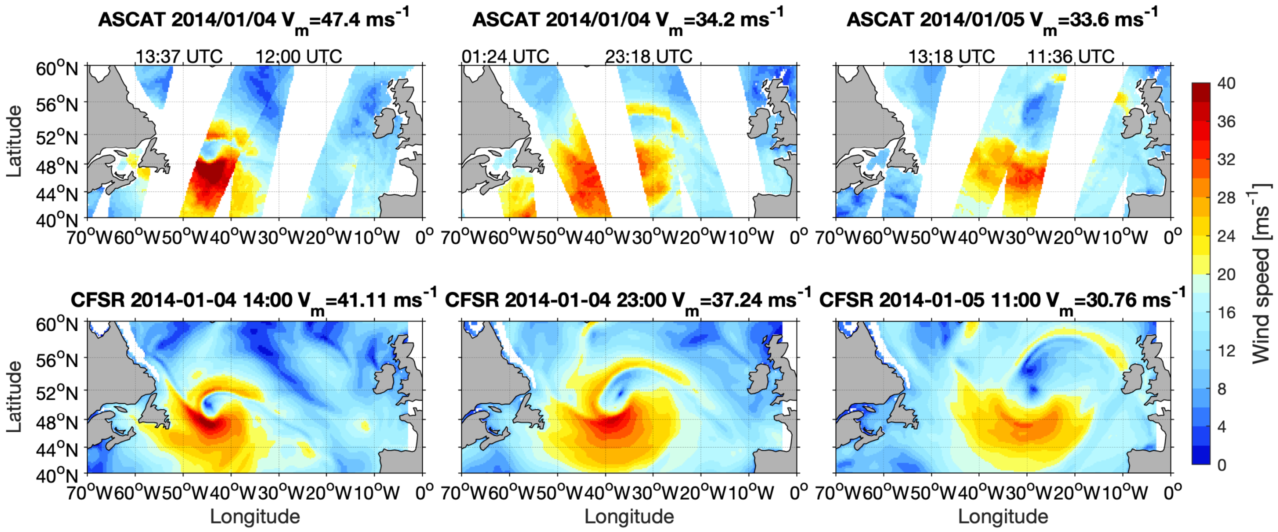

Figure S8. Comparison of wind speeds between ASCAT scatterometer and CFSR during January 4-5, 2014. The ASCAT $0.25^o \times 0.25^o$ gridded data were obtained from http://www.remss.com/missions/ascat/.

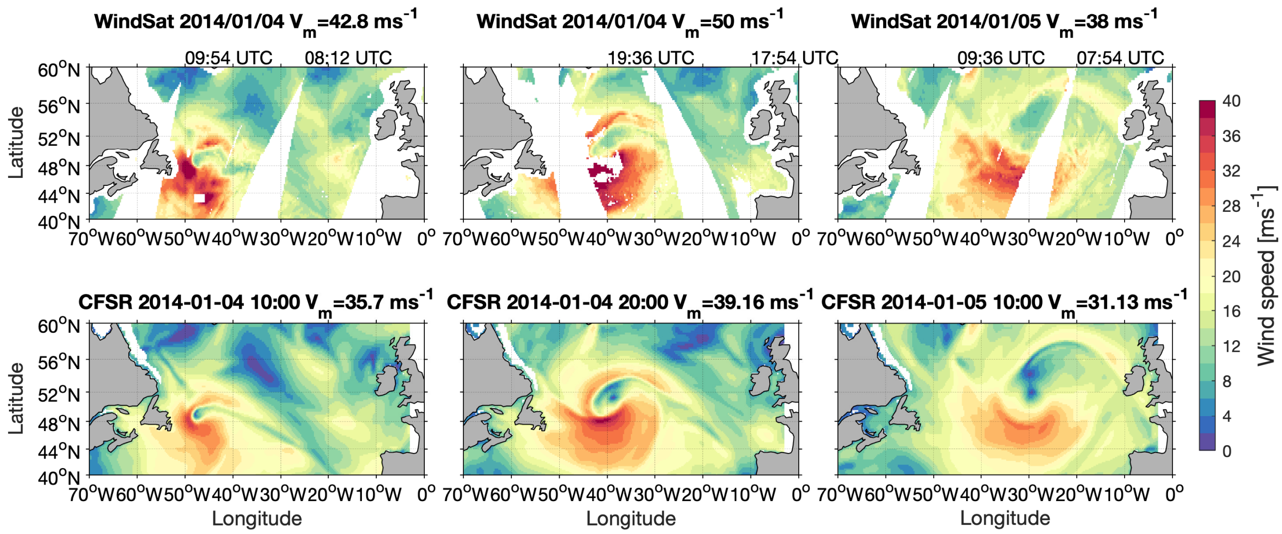

Figure S9. Comparison of wind speeds between WindSat radiometer based measurements and CFSR during January 4-5, 2014. The WindSat $0.25^o \times 0.25^o$ gridded data were obtained from http://www.remss.com/missions/windsat/.

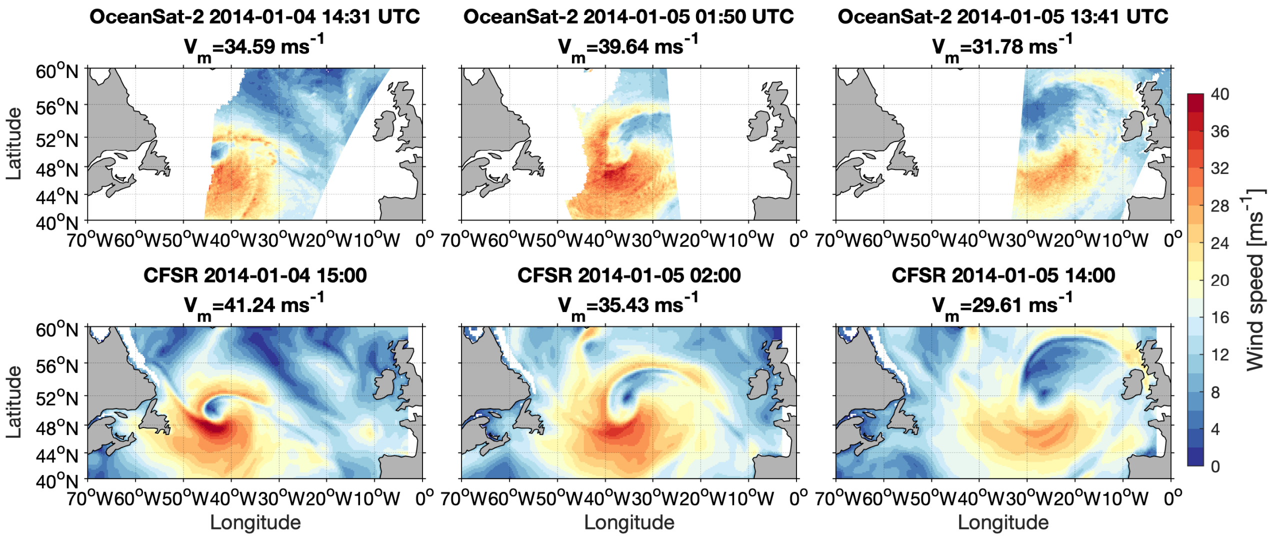

Figure S10. Comparison of wind speeds between OceanSat-2 scatterometer based measurements and CFSR during January 4-5, 2014. The OceanSat-2 L2 data were obtained from PODAAC/NASA.

Table S2. Data used in this paper and their sources

Data	URL
Reanalysis and hindcast	
ERA5/ECMWF	https://cds.climate.copernicus.eu/cdsapp#!/home
IOWAGA/IFREMER	ftp://ftp.ifremer.fr/ifremer/ww3/HINDCAST/GLOBAL/
Satellite altimeter	
Ribal and Young (2019)	https://portal.aodn.org.au/
Globwave/IFREMER	http://globwave.ifremer.fr/
PODAAC/NASA	https://podaac.jpl.nasa.gov/
In-situ	
UK Met Office buoy	http://www.marineinsitu.eu/dashboard/
Satellite wind products	
Widsat	http://www.remss.com/missions/windsat/
ASCAT	http://www.remss.com/missions/ascat/
OceanSat-2	https://podaac.jpl.nasa.gov/
Wind and sea ice concentration	
CFSR/NCEP	https://rda.ucar.edu/datasets/ds093.1/
CFSv2/NCEP	https://rda.ucar.edu/datasets/ds094.1/